

Boundary between hadron and quark-gluon structure of nuclei

H. J. Pirner and J. P. Vary

*Institut für Theoretische Physik der Universität Heidelberg, Germany, and**Department of Physics and Astronomy, Iowa State University, Ames, Iowa 50011, USA*

(Received 7 September 2010; revised manuscript received 20 April 2011; published 6 July 2011)

We show that the boundary between quark-dominated and hadron-dominated regions of nuclear structure may be blurred by multinucleon quark clusters arising from color percolation. Recent experiments supporting partial percolation in cold nuclei and full percolation in hot/dense nuclear matter include deep inelastic lepton-nucleus scattering, relativistic heavy-ion collisions, and the binding energy in ${}^5\text{He}_\Lambda$.

DOI: [10.1103/PhysRevC.84.015201](https://doi.org/10.1103/PhysRevC.84.015201)

PACS number(s): 25.30.Fj, 21.80.+a, 25.75.Ag

I. INTRODUCTION

Heavy-ion experiments and lattice-gauge simulations of quantum chromodynamics (QCD) intensively investigate the quark-gluon phase transition relevant to the early universe. Another challenge is to understand, under varying external conditions, the roles of fundamental quarks and gluons in hadronic and nuclear matter. Where are they essential to replace low-energy descriptions of nuclei based on hadrons (neutrons, protons, and mesons)? From lattice QCD simulations, we understand quantitatively the masses of the hadrons. Similarly, we know that quark and gluon color charges make the strong coupling constant grow at distances larger than the hadron size and generate their own confinement within color-neutral hadrons. However, a theoretical understanding of longer-range QCD dynamics, beyond the size of a hadron, is still a challenge for lattice simulations. We present evidence for an intermediate-range phenomena, the formation of multi-quark clusters in cold and hot equilibrated baryonic matter that blurs the boundary between the hadron and quark-gluon phases.

We adopt classical percolation theory [1–4] to bridge the gap between quark and hadron physics. In our hybrid approach we take nuclear matter to be composed of color neutral clusters, which consist at zero temperature of 3, 6, 9, 12, $q \dots$ quarks and at finite temperature we include quark-antiquark ($q\bar{q}$) states for the mesons. These larger units have small probabilities in cold nuclei, but are conducting color, like subdomains of ionized plasma in an electrically neutral gas. We assume there is a common size parameter for the lowest mass nucleon and pion that determines the overlap of hadronic states at finite density and consequently the probabilities to form these multihadron clusters. We expect the presently neglected gluon content of these systems to become important at very short distances.

In Fig. 1 we summarize the percolation approach to nuclear physics where, between the well-established hierarchy of quark-gluon physics and nucleon-meson physics, we insert a new layer consisting of color neutral multi-quark clusters. Percolation theory allows us to connect these regions and appears sufficient to unify the microscopic and macroscopic physics with an accuracy of $\approx 10\%$. Solutions for cluster probabilities in nuclei have previously been reported [4,5]. Current experiments probe nuclei with high resolution and/or high excitation energies where this quark-clustering layer becomes

manifest as we now discuss. Future electron-nucleus (e - A) experiments at the Thomas Jefferson National Accelerator Facility (JLab) with 12 GeV could enhance the resolution by an order of magnitude and reveal precise cluster details.

II. DEEP INELASTIC SCATTERING ON NUCLEI WITH $x > 1$

For deep inelastic lepton-nucleus scattering, in a Born approximation, the Bjorken-variable $x = \frac{Q^2}{2m_N\nu}$ (Q is the magnitude of the four-momentum transfer to the target, ν is the laboratory energy loss of the lepton, and m_N is the nucleon mass) measures the fraction of the struck quark's momentum relative to the nucleon momentum. Therefore, a constituent of an isolated nucleon carries $x \leq 1$. Quark clustering in nuclei leads to a simple prediction for the region $x > 1$ where cooperative effects are required to provide scattering support.

Following our previous work [3], we assume that the nucleus consists of 3, 6, 9, 12, ... quark clusters with definite internal structure (i.e., defined structure functions) and cluster probabilities are governed by intermediate-range correlations evaluated with realistic correlated wave functions for $A \leq 4$ nuclei and then scaled according to average density for heavier nuclei [4]. We omit effects of additional strong density fluctuations due to, for example, α -cluster formation in $A > 4$ nuclei. Two nucleons form a 6-quark cluster when they are separated by less than a critical distance $d_c = 2R_c = 1$ fm, where R_c is a nucleon's critical "color percolation" radius. A third nucleon with separation less than d_c from the previous two then joins to make a 9-quark cluster, etc. The probability $p_i(A)$ that a quark selected at random in nucleus A originates from an i -quark cluster (for $i = 6, 9, 12, \dots$) decreases rapidly with increasing quark number. It follows that the e - A structure functions are determined by the 6-quark cluster for $1 < x < 2$ and by the 9-quark cluster for $2 < x < 3$. Independent of the cluster structure functions, per nucleon ratios of deep inelastic cross sections in two nuclei A and B will be constant in the respective x intervals and reflect only the ratio of cluster probabilities of these nuclei, i.e., for $1 < x < 2$,

$$\frac{(1/A)d\sigma/dxdQ^2(eA)}{(1/B)d\sigma/dxdQ^2(eB)} = \frac{p_6(A)}{p_6(B)}, \quad (1)$$

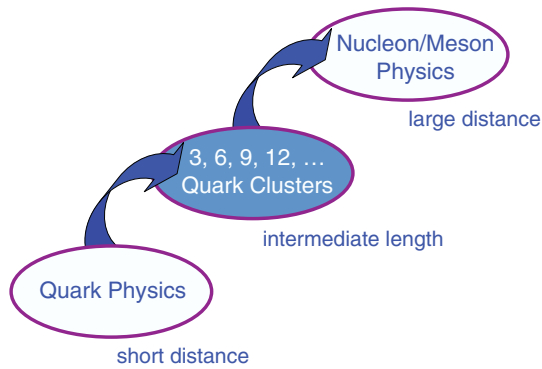


FIG. 1. (Color online) The separation of quark physics, the physics of color neutral multi-quark clusters, and nucleon/meson physics.

and for $2 < x < 3$,

$$\frac{(1/A)d\sigma/dxdQ^2(eA)}{(1/B)d\sigma/dxdQ^2(eB)} = \frac{p_9(A)}{p_9(B)}, \quad (2)$$

and so forth for larger clusters. We have shown how this model successfully describes the inclusive inelastic cross sections on deuterium in the region $1 < x < 2$ [6] when the 6-quark cluster component is included.

The intense JLab electron beam has allowed these suppressed regions of phase space to be measured [7]. In Fig. 2 we show the measured ratio (discrete points) [7] of per nucleon responses of ^{56}Fe to ^{12}C together with our predictions (horizontal bars) [4] in the 6-quark cluster region $1 < x < 2$ and the 9-quark cluster region $2 < x < 3$. We estimate the theoretical ratios have 10% uncertainty. In the former kinematic region the experimental ratio for ^{56}Fe to ^{12}C is $1.17 \pm 0.04 \pm 0.11$ [7] in good agreement with our theoretical prediction of 1.17 ± 0.12 . The experimental ratio above $x = 2$ is quoted [7] as 1.44 with about 33% uncertainty which agrees with our theoretical ratio of 1.39 ± 0.14 .

Although we derive encouragement from the agreement (within large uncertainties) for the ratio in the 9-quark cluster region we believe this agreement may be accidental for two reasons. First, the large x values in these experiments come with rather small energy transfer ν in the rest system of the nucleus. If one translates these ν values into a time resolution then one finds that this “snapshot” has a rather long exposure time, namely, about $\Delta t = 1/0.3 \text{ GeV} = 0.7 \text{ fm}/c$. Therefore, the short-lived fluctuation of a 9-quark clusters may be represented only partially in the $2 < x < 3$ cross section. Future e - A experiments with new or upgraded facilities can elucidate the dependence on exposure times. They would also allow higher momentum transfer Q , which suppresses the coherent effects of quasielastic quark-cluster knockout [3] at $x = 1, 2$, etc., which may be visible in Fig. 2. Second, the calculations [4] were performed without three-nucleon (NNN) interactions since they were unavailable at that time. NNN correlations should reflect the repulsive NNN force and suppress 9-quark probabilities overall. Due to their intermediate range, we expect the NNN force will also lead to nontrivial A -dependent effects. These complications motivate

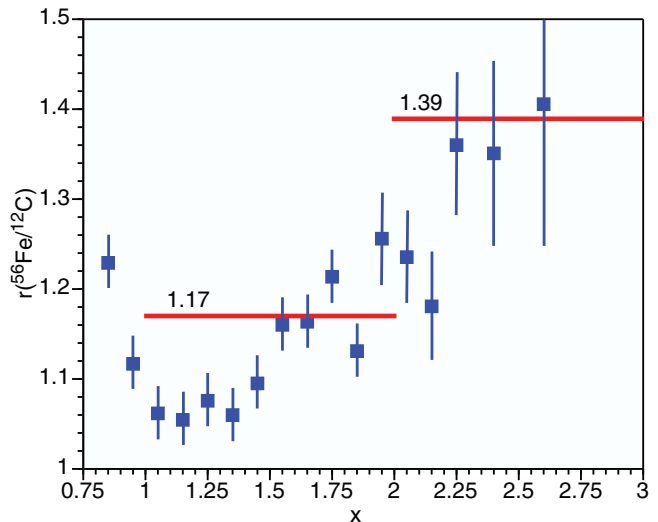


FIG. 2. (Color online) JLab data for the ratio of per nucleon responses of ^{56}Fe to ^{12}C over a range of Bjorken $x_B = x$ that exceeds unity [7], the limit for data on an isolated nucleon. We note there is a data point, $r = 2.2$ at $x = 2.8$, which is far off the vertical scale. Multiquark clusters support a nuclear response above $x = 1$. The horizontal lines show the theoretical predictions (1.17 and 1.39) for regions dominated by 6- and 9-quark clusters, respectively [4].

significant theoretical effort to modernize the quark-cluster probability calculations.

An alternative interpretation [8] of these deep inelastic scattering data employs short-range two-nucleon (NN) correlations to generate very high ($\approx 1 \text{ GeV}/c$) nucleon relative momenta so that the struck quark may obtain a large momentum and exceed the kinematical boundary $x = 1$. The high momenta are obtained by strongly repulsive short-range NN -potentials acting at separation distances of $r < 0.7\text{--}0.8 \text{ fm}$. In so far as this nucleon-based approach generates similar kinematics, it may appear to represent a nonrelativistic picture dual to our quark-cluster approach. However, color-conducting multi-quark clusters offer both a relativistic approach and additional experimental consequences. For example, virtual photons at high resolution can peer into the quark-cluster zone of color conductivity and measure details of the quark-cluster structure functions. We may discover, for example, that percolating quarks carry less of the total momentum sum rule than isolated nucleons even though $x > 1$ regions are populated. This seems plausible on the basis of elementary physics since the color confining region is enlarged in the 6-quark cluster [9].

A recent experiment probing the $x < 1$ region suggests that, while ^3He , ^4He , and ^{12}C responses follow a density scaling trend, the ^9Be response does not [10]. In addition, a detailed study of hadron-nucleus data at $x > 1$ shows significant deviations from simple density scaling for ^6Li and ^7Li nuclei [11]. We understand these Li and Be anomalies as motivating the inclusion of α -clustering effects which are expected to be especially significant for these nuclei. For this reason and our neglect of NNN potentials, we prefer to focus on larger systems that we believe are less sensitive to these corrections.

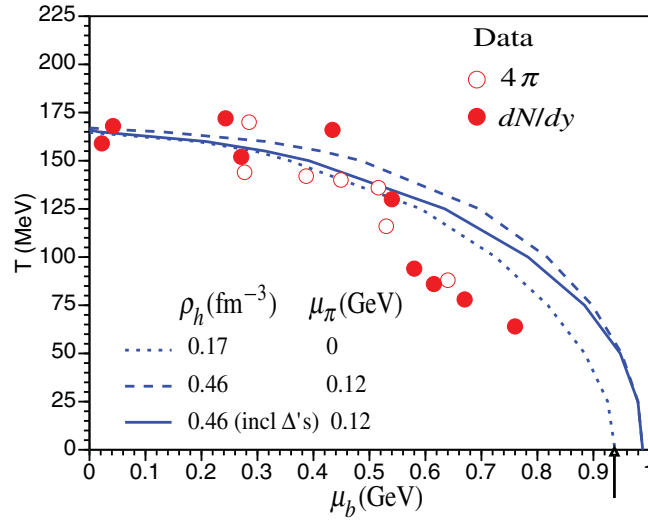


FIG. 3. (Color online) The boundary between hadron matter and quark-gluon matter from our quark percolation model for 50% percolation rate (upper curve) and 22% percolation rate (lower curve) in a temperature T versus baryon chemical potential μ_b phase diagram. The parameters of the three theory curves are specified in the legend. The arrow indicates μ_b for nuclear matter at $T = 0$. The freeze-out data are compiled from different experiments [13].

III. RELATIVISTIC HEAVY-ION COLLISIONS

We now show that the quark-cluster description is appropriate at high excitation energies produced in relativistic heavy-ion collisions. Cluster probabilities are mainly a function of the local hadron density and, to proceed to finite temperature, we introduce a pion component. We assume that the critical separation distance for the pions to transition into larger quark clusters is the same as for nucleon percolation, $d_c = 1$ fm, and that d_c is temperature independent. Therefore we adjust the baryon chemical potential so that the sum of the baryon and pion densities is the same as the density of baryons at $T = 0$ to maintain approximately constant color percolation probability. Then

$$\rho_{\text{hadrons}}(\mu, T) = \rho_{\text{baryons}}(\mu_b, T) + \rho_{\text{pions}}(\mu_\pi, T). \quad (3)$$

We set the pion chemical potential $\mu_\pi = 0$ at $T = 0$ to fix the reference baryon chemical potential μ_b at normal nuclear matter density 0.17 baryons/fm³ (Fermi momentum $k_f = 1.36$ fm⁻¹). The nucleon dispersion relation is influenced by the nuclear mean-field potential for which we take [12]

$$\epsilon(k) = \sqrt{(k^2 + (m_N + V_s(k))^2) + V_0(k)}, \quad (4)$$

where the scalar and vector self-energies are momentum dependent:

$$V_s(k) = -0.35 \text{ GeV} [1 - 0.05(k/k_f)^2], \quad (5)$$

$$V_0(k) = +0.29 \text{ GeV} [1 - 0.05(k/k_f)^2]. \quad (6)$$

The freeze-out data [13] extracted from heavy-ion collisions at high temperatures are shown in Fig. 3 as a function of T and μ_b along with the theoretical (dotted) curve which corresponds

to a mostly hadronic system of pions and nucleons. On this curve, each quark is percolating 22% of the time in $i > 3$ -quark clusters. We also plot in Fig. 3 a curve with a higher percolation rate which we call “percolating nuclear matter” and find μ_b where more than 50% of all nucleons have transitioned to 6, 9, 12,...-quark clusters at $T = 0$. This $T = 0$ state requires $\rho_{\text{baryon}} = 0.46$ fm⁻³, i.e., 2.7 times nuclear density, and therefore has a larger chemical potential than nuclear matter. For this case, we also adopted $\mu_\pi = 120$ MeV, used to fit the transverse momentum dependence of the pion spectra from a kinetically equilibrated pion distribution [14]. Taking into account also the Δ resonance at 1.236 GeV shifts the higher temperature percolation curve (solid line) toward the curve corresponding to nuclear matter density (dotted line).

The percolation model is a geometrical model and is not sensitive to the decay properties of resonances, but more to the number of hadronic states in a certain volume. The classical percolation transition is a cross over transition in finite systems and the transition itself is not well defined. Thus quark percolation blurs the boundary between the hadron phase and the quark-gluon phase.

IV. EXTENDED QUARK ORBITALS IN HYPERNUCLEI

Another avenue to explore quark-cluster structures is to replace one of the nucleons with a strange spectator, a Λ hyperon, producing a hypernucleus. The successful explanation of the hypernucleus spin-orbit potential based on quark dynamics [15] motivates a closer look at possible quark-cluster effects. In particular, we focus on a longstanding puzzle [16] of the sudden decrease of the binding energy in ${}^5\text{He}_\Lambda$ compared with the binding energy of a baryon-based calculation with two-body forces. The ${}^4\text{He}$ nucleus is doubly magic in the language of the shell model with protons and neutrons but the full occupation of the $0s$ state by protons and neutrons does not preclude the addition of a Λ hyperon to the $0s$ state. With two-body forces alone one then obtains overbinding of the $A = 5$ hypernucleus by 1–3 MeV. One way out is through effective many-baryon potentials. Indeed, calculations with purely baryonic degrees of freedom and a three-body Λ - NN force resulting from an explicit Σ component in the wave function [17] seem to show the repulsive character for the total three-body contributions. However, if the 3-quark substructure of the Λ matters, i.e., up (u) + down (d) + strange (s), then for the 12-quark cluster configuration of ${}^4\text{He}$, the Λ 's up and down quarks cannot occupy the $0s$ shell which can accommodate only 12 u and d quarks according to the Pauli principle. The observation of such extended quark orbitals would be the best proof for color percolation in nuclei as Baym [1] has already indicated in 1979.

Let us make a simple estimate of this effect. The mean spacing in the constituent quark shell model would be larger by a factor of 3 based on the ratio of nucleon to constituent quark masses

$$\hbar\omega_Q = 3\hbar\omega_N = 75 \text{ MeV} \quad (7)$$

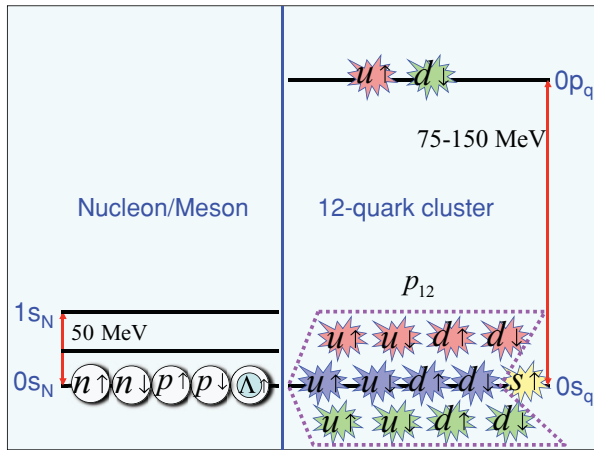


FIG. 4. (Color online) Sketch of the two possible views of the Λ attached to the the lowest configuration of two neutrons (n) and two protons (p). On the left, the Λ and the nucleons are structureless baryons with spin projections indicated. On the right, their quark substructure is taken into account with spin and color attributes sketched. In the latter case, the 12-quark cluster configuration that appears with probability $p_{12} = 0.007$ in the quark-cluster model, forces the up (u) and down (d) quarks of the Λ to be in the next higher, Pauli-allowed, orbit $0p_q$. The Λ 's strange (s) quark may occupy the lowest $0s_q$ level.

Including a size factor for the smaller 12-quark cluster compared to the nuclear size could easily boost this mean spacing by a factor of 2.

Therefore a 12-quark cluster with 2 extra u and d quarks would need an extra excitation energy of approximately 150–300 MeV. Our quark-cluster model provides [4] $p_{12}(^4\text{He}) = 0.007$, a small probability for such an extended 12-quark cluster in ^4He (Fig. 4). Multiplying this probability with the Pauli-required u - and d -quark excitations of 150–300 MeV would give a decrease in $^5\text{He}_\Lambda$ binding of 1–2 MeV, in rough

agreement with experiment. This one case is not sufficient to establish the existence of extended quark shell model states. One should look at heavier hypernuclei where the additional Λ has to split up in a low-lying s quark and an excited ud pair. Future precision experiments could explore the binding energy systematics of heavier closed shell systems such as $^{16}\text{O}_\Lambda$, $^{17}\text{O}_\Lambda$ and $^{16}\text{N}_\Lambda$, $^{17}\text{N}_\Lambda$.

Additional experimental tests of quark clustering can be performed such as measuring high-mass di-lepton pair production from nuclear targets [18] (Drell-Yan process).

If one asks whether our understanding of QCD is complete, the question may be recast to whether additional theoretical or experimental work can improve the situation decisively. Compressed baryonic matter [19] is an area where our theoretical and experimental understanding is not as well developed as baryon-free matter. For nuclei a theory which contains nucleons and multi-quark cluster states is an efficient way to describe the transition from purely nucleonic matter to quark matter at high baryon density. A hybrid model with quark clusters would define a major advance if one would be able to rewrite the smooth infrared limit of lattice QCD in a field theoretic continuum picture. Such a picture should also continue the phase diagram into the totally percolated phase where perhaps the formation of a qq -dimer condensate [20] and BCS pairing [21] of quarks can be found in analogy to the physics of cold atoms. Quark percolation and these other features of the QCD phase diagram would also impact astrophysics.

ACKNOWLEDGMENTS

We thank V. Burkert for providing the JLAB experimental data [7]. We acknowledge valuable discussions with V. Burkert, W. Brooks, S. Coon, J. Knoll, R. J. Peterson, J. Stachel, and B. Povh. This work was supported in part by USDOE Grant DE-FG-02-87ER40371 and, in part, by the Alexander von Humboldt Foundation.

- [1] G. Baym, *Physica A* **96**, 131 (1979); G. Baym, *Prog. Nucl. Part. Phys.* **8**, 73 (1982).
- [2] H. Satz, *Nucl. Phys. A* **642**, 130 (1998).
- [3] H. J. Pirner and J. P. Vary, *Phys. Rev. Lett.* **46**, 1376 (1981).
- [4] M. Sato, S. A. Coon, H. J. Pirner, and J. P. Vary, *Phys. Rev. C* **33**, 1062 (1986).
- [5] F. Guttner and H. J. Pirner, *Nucl. Phys. A* **457**, 555 (1986); R. Boisgard, J. Desbois, J. F. Mathiot, and C. Ngo, *ibid.* **489**, 731 (1988).
- [6] G. Yen, J. P. Vary, A. Harindranath, and H. J. Pirner, *Phys. Rev. C* **42**, 1665 (1990).
- [7] K. S. Egiyan *et al.*, *Phys. Rev. Lett.* **96**, 082501 (2006).
- [8] L. Frankfurt, M. Sargsian, and M. Strikman, *Int. J. Mod. Phys. A* **23**, 2991 (2008).
- [9] O. Nachtmann and H. J. Pirner, *Z. Phys. C* **21**, 277 (1984).
- [10] J. Seely *et al.*, *Phys. Rev. Lett.* **103**, 202301 (2009).
- [11] R. J. Peterson, *Nucl. Phys. A* **791**, 84 (2007).
- [12] B. Chen and Z. Ma, *Phys. Lett. B* **339**, 297 (1994).
- [13] A. Andronic, P. Braun-Munzinger, and J. Stachel, *Nucl. Phys. A* **772**, 167 (2006).
- [14] P. Gerber, H. Leutwyler, and J. L. Goity, *Phys. Lett. B* **246**, 513 (1990).
- [15] H. J. Pirner and B. Povh, *Phys. Lett. B* **114**, 308 (1982).
- [16] E. V. Hungerford and L. C. Biedenharn, *Phys. Lett. B* **142**, 232 (1984).
- [17] H. Nemura, Y. Akaishi, and Y. Suzuki, *Phys. Rev. Lett.* **89**, 142504 (2002).
- [18] A. Harindranath and J. P. Vary, *Phys. Rev. D* **34**, 3378 (1986).
- [19] B. Friman, C. Höhne, J. Knoll, S. Leupold, J. Randrup, R. Rapp, and P. Senger (Eds.), *The CBM Physics Book: Compressed Baryonic Matter in Laboratory Experiments*, Lecture Notes in Physics (Springer-Verlag, New York, 2011).
- [20] A. H. Rezaeian and H. J. Pirner, *Nucl. Phys. A* **779**, 197 (2006).
- [21] T. Schäfer and F. Wilczek, *Phys. Rev. D* **60**, 114033 (1999).